

An analytic model for the optical properties of gold

P. G. Etchegoin,^{a)} E. C. Le Ru,^{b)} and M. Meyer

The MacDiarmid Institute for Advanced Materials and Nanotechnology, School of Chemical and Physical Sciences, Victoria University of Wellington, P.O. Box 600, Wellington, New Zealand

(Received 1 August 2006; accepted 11 September 2006; published online 24 October 2006)

[DOI: [10.1063/1.2360270](https://doi.org/10.1063/1.2360270)]

The importance of gold (Au) as a substrate in biotechnology (and in the form of nanoparticles of different types¹) cannot be underestimated. Gold plays an important role in a myriad of plasmonics-type spectroscopies [such as surface enhanced raman scattering (SERS)] where it is widely preferred for biological applications over silver (Ag) for its relatively easier surface chemistry, the possibility of attaching molecules via thiol groups, good biocompatibility, and chemical stability. The optical properties of silver in the visible/near-uv range are fairly well represented by a simple Drude model, and several parametrizations of the dielectric function $\epsilon(\omega)$ have appeared in the literature² and have been used subsequently for different simulations.³ One could argue that an analytic model for $\epsilon(\omega)$ is not really necessary, and that it is always possible to resort to interpolations of the experimental data. However, the advantages of having a realistic analytic representation of $\epsilon(\omega)$ with a small number of physically meaningful parameters are self-evident, not only for simulations but also to understand situations where the intrinsic parameters of the metal might be modified by external perturbations.

Compared to Ag, the optical properties of Au are more difficult to represent in the visible/near-uv region with an analytic model. The reason for that is the more important role in the latter played by interband transitions in the violet/near-uv region. Au has at least two interband transitions at $\lambda \sim 470$ and ~ 330 nm that do play an important role and must be included explicitly if a realistic analytic model for $\epsilon(\omega)$ is sought. Their line shapes (coming from the joint density of states of the interband transitions⁴) are not very well accounted for by a simple Lorentz oscillator (as in a simple molecular transition), and attempts to add simple Lorentz oscillators to a Drude term to account for the interband transitions very rapidly face limitations.⁵ The reason for this is that the transitions have a somewhat asymmetric line shape than could only be accounted for with simple Lorentz oscillators by adding a series of additional “artificial” transitions, with the consequent increase in the number of (mostly unphysical) parameters. It is clear that with a sufficiently large number of Lorentz oscillators *any* line shape can be modeled, but the parameters of the model are then ill defined and have no real meaning; they do not provide more insight than a (equally unphysical) fit with high-degree polynomial, or a simple numerical interpolation of the experimental data.

A different type of analytic model for the two interband transitions in gold in the violet/near-uv region has to be included to achieve a reasonable representation of $\epsilon(\omega)$ with a

minimum set of parameters. It is possible to include a family of analytical models (called critical points) for transitions in solids, which satisfy a set of minimum requirements (like Kramers-Kronig consistency) and reproduce most of the line shapes in $\epsilon(\omega)$ observed experimentally. Critical point analysis of interband transitions in $\epsilon(\omega)$ is a subject with a long-standing tradition in semiconductors.⁶

Following this approach, the frequency-dependent optical properties of Au in the visible/near-uv range can be very well represented by an analytic formula with three main contributions, to wit,

$$\epsilon_{\text{Au}}(\omega) = \epsilon_{\infty} - \frac{\omega_p^2}{(\omega^2 + i\Gamma\omega)} + G_1(\omega) + G_2(\omega), \quad (1)$$

where the first and second terms are the standard contribution of a Drude model⁷ with a high-frequency limit dielectric constant ϵ_{∞} , a plasma frequency ω_p , and a damping term Γ , while $G_1(\omega)$ and $G_2(\omega)$ are the contributions from the aforementioned interband transitions (gaps). For the latter, we use the critical point transitions described in Ref. 8, namely,

$$G_i(\omega) = C_i [e^{i\phi_i}(\omega_i - \omega - i\Gamma_i)^{\mu_i} + e^{-i\phi_i}(\omega_i + \omega + i\Gamma_i)^{\mu_i}], \quad (2)$$

where the symbols have the following meaning: (i) C_i , amplitude; (ii) ϕ_i , phase; (iii) ω_i , energy of the gap; (vi) Γ_i , broadening; and (v) μ_i , order of the pole. For $\omega \approx \omega_i$ the second term in (2) is less important than the first (it is the contribution from the pole in the negative frequency axis in the complex plane), but it needs to be added to the first term to ensure an expression which is fully Kramers-Kronig consistent. We assume throughout that the temporal variation of all fields goes as $\exp(-i\omega t)$; the opposite sign implies a change in the sign of the imaginary part of $\epsilon(\omega)$ and is the convention mostly used in engineering. As explained in Ref. 8, critical points like (2) have the only drawback that they do not satisfy the “plasma sum rule” but this is not a limitation when they are used over a finite frequency range. The order of the poles (μ_i) needs to be decided for each gap. In principle, the order is connected to the dimensionality of the Van Hove singularity in the joint density of states for the interband transitions.⁴ In practice, however, many features in the dielectric function of solids involving several close transitions (and affected by broadening and limited experimental resolution) can be represented equally well by poles of more than one order. A pragmatic approach is to start with simplest order poles until a desired accuracy is obtained. The meaning

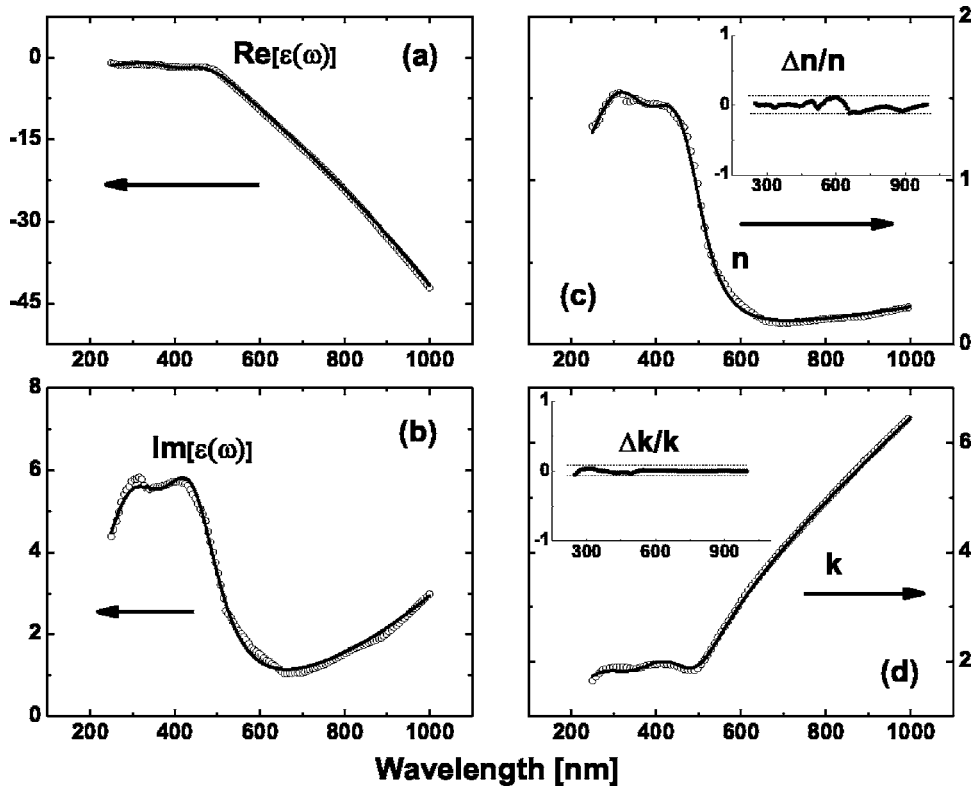


FIG. 1. (a) and (b) show the real and imaginary parts of the dielectric function of Au while (c) and (d) show the corresponding real (n) and imaginary (k) parts of the complex index of refraction. The data points are the experimental values from Johnson and Christy (Ref. 9) while the solid lines are the fitted results with Eq. (3). The parameters obtained from the fits are given in Table I. For n and k we show the normalized spectral difference between the experimental values and the model ($\Delta n/n$ and $\Delta k/k$); the differences with the data of Johnson and Christy (Ref. 9) are never higher than 12% for n and much smaller (4%) for k .

and values of ω_i and Γ_i will not change radically by the exact choice of μ_i anyway.

For the two interband transitions in Au we choose $\mu_1 = \mu_2 = -1$ and achieve a satisfactory representation of the experimental $\epsilon(\omega)$. It is convenient also to change to a wavelength dependent dielectric function (most commonly found in spectroscopy). We used the following definitions: (i) $\lambda = 2\pi c/\omega$ (with c =speed of light), (ii) $\lambda_p = 2\pi c/\omega_p$ (plasma wavelength), (iii) $\gamma_p = 2\pi c/\Gamma$ (damping expressed as a wavelength), (iv) $\lambda_i = 2\pi c/\omega_i$ (interband transition wavelength), (v) $\gamma_i = 2\pi c/\Gamma_i$ (transition broadenings expressed as wavelengths), and $A_i = C_i/\omega_i$ (dimensionless critical point amplitudes). The full model dielectric function of Au as a function of λ then reads

$$\epsilon_{\text{Au}}(\lambda) = \epsilon_{\infty} - \frac{1}{\lambda_p^2(1/\lambda^2 + i/\gamma_p\lambda)} + \sum_{i=1,2} \frac{A_i}{\lambda_i} \left[\frac{e^{i\phi_i}}{(1/\lambda_i - 1/\lambda - i/\gamma_i)} + \frac{e^{-i\phi_i}}{(1/\lambda_i + 1/\lambda + i/\gamma_i)} \right]. \quad (3)$$

The first line in Eq. (3) is the Drude contribution, while the second accounts for the two interband transitions. Unlike simple Lorentz oscillators, the chosen critical points allow for an easy adjustment of an asymmetric line shape.¹¹ The parametrization in Eq. (3) is fitted and compared in Fig. 1 to one of the most widely available data sets in the literature for the optical properties of Au, coming from the paper of Johnson and Christy.⁹ Similar results are obtained if the real and imaginary parts of either $\epsilon(\omega)$ or the complex index of refraction ($\tilde{n}(\omega) = n + ik = \sqrt{\epsilon(\omega)}$) are fitted. Figure 1 shows

the overall agreement with both $\epsilon(\omega)$ and $\tilde{n}(\omega) = n + ik$. The parameters for Eq. (3) from the fit are displayed in Table I. Note that we simplified the values of the phases. The fit with all free parameters produces by itself $\phi_1 \sim \phi_2 \sim -\pi/4$. We therefore fixed the two phases to be the same and equal to $-\pi/4$ to have one parameter less and improve the convergence of the others.

It should be emphasized that there are variations in the reported optical properties of Au in the literature depending on the source.¹⁰ This is particularly crucial in the region of the interband transitions and most of the time more evident in the imaginary part of $\epsilon(\lambda)$. Most of these differences can be tracked down to experimental problems. In situations where coupling to surface plasmons is possible, the optical properties of metals are very susceptible to imperfections. Details such as the “surface texture” of the sample or the exact experimental technique used (ellipsometry, combina-

TABLE I. Parameters in Eq. (3) to reproduce the data of Johnson and Christy (Ref. 9) shown in Fig. 1.

Parameter (units)	Data of Johnson and Christy (Ref. 9)
ϵ_{∞}	1.53
λ_p (nm)	145
γ_p (nm)	17 000
A_1	0.94
ϕ_1 [rad]	$-\pi/4$
λ_1 (nm)	468
γ_1 (nm)	2300
A_2	1.36
ϕ_2 (rad)	$-\pi/4$
λ_2 (nm)	331
γ_2 (nm)	940

tion of absorption and reflection, etc.) will have an influence on the final outcome. The parameters in Table I should not be taken as completely universal but rather as a good starting point to approximate the optical properties of gold in most simulations and, in particular, to reproduce the data of Johnson and Christy with an analytic model. Therefore, most differences found in the published data are, in general, not due to experimental errors but to differences in the polycrystallinity and packing fractions of the samples. It is known that the different data can usually be brought into reasonable agreement by means of the Bruggeman effective-medium theory,¹² possibly supplemented by grain-boundary scattering effects on the carrier lifetime. Our results, therefore, can be made more generally applicable by using the Bruggeman effective-medium expression to adjust the void fractions.¹²

Several experimental techniques to do with plasmons require sometimes that a specific resonance condition is met (for example, $\text{Re}[\epsilon(\omega)] = -1$ or -2 for the resonance of a cylinder or sphere in air, respectively). In complex experimental situations (in particular, if the texture and geometry of the metallic object are not well controlled), the exact resonance conditions will have to be adjusted according to the case at hand. From the modeling standpoint, however, Eq. (3) with the parameters in Table I should provide everything that is required for the local dielectric function $\epsilon(\lambda)$ of Au and should capture the essence of any plasmonic effect compatible with the validity of the specific modeling. As it is done for semiconductors,⁶ a physical parametrization of the dielectric function of Au like Eq. (3) also opens the door to the study of how these parameters might vary under the presence of external perturbations, providing a physical background for their interpretation.¹³ This is not possible obviously in parametrizations with a large number of unphysical transitions (Lorentz oscillators) which artificially account for asymmetric line shapes rather than real optical transitions.

A Drude contribution from free electrons needs two parameters (plasma frequency and damping) and each interband transition needs a minimum of four parameters (gap energy, broadening, phase, and amplitude). Together with the

high-frequency limit of the dielectric function (ϵ_{∞}) this makes a total (minimum) of 11 parameters (given in Table I) to obtain a physical representation of $\epsilon(\lambda)$ in Au. For the data of Johnson and Christy we find that the phase of the two interband transitions can be fixed to be the same, reducing the number of total parameters to 10. This might not be true for data from other sources.

The main result of this short Note is the model dielectric function given by Eq. (3), supplemented with the parameters in Table I, which reproduces one of the best known data sets for the experimental dielectric function of Au (as exemplified in Fig. 1) with an analytic expression with physical parameters.

We are indebted to Mark Clarkson (Industrial Research Limited, Lower Hutt, New Zealand) for valuable discussions and help with ellipsometry.

^aElectronic mail: pablo.etchegoin@vuw.ac.nz

^bElectronic mail: eric.leru@vuw.ac.nz

¹J. B. Jackson, S. L. Westcott, L. R. Hirsch, J. L. West, and N. J. Halas, *Appl. Phys. Lett.* **82**, 257 (2003).

²R. Rojas and F. Claro, *J. Chem. Phys.* **98**, 998 (1993).

³P. G. Etchegoin and E. C. Le Ru, *J. Phys.: Condens. Matter* **18**, 1175 (2006).

⁴P. Y. Yu and M. Cardona, *Fundamentals of Semiconductors: Physics and Materials Properties* (Springer, Berlin, 2004).

⁵L. Novotny and B. Hecht, *Principles of Nano-Optics* (Cambridge University Press, Cambridge, 2006), p. 383.

⁶P. Etchegoin, J. Kirchner, and M. Cardona, *Phys. Rev. B* **47**, 10292 (1993).

⁷M. Born and E. Wolf, *The Principles of Optics* (Pergamon, Oxford, 1964).

⁸J. Leng, J. Opsal, H. Chu, M. Senko, and D. E. Aspnes, *Thin Solid Films* **313–314**, 132 (1998).

⁹P. B. Johnson and R. W. Christy, *Phys. Rev. B* **6**, 4370 (1972).

¹⁰E. D. Palik, *Handbook of Optical Constants of Solids III* (Academic, New York, 1998).

¹¹M. Campoy-Quiles, G. Heliotis, R. Xia, M. Ariu, M. Pintani, P. G. Etchegoin, and D. D. C. Bradley, *Adv. Funct. Mater.* **15**, 925 (2005).

¹²D. E. Aspnes, *Am. J. Phys.* **50**, 704 (1982).

¹³M. A. van Dijk, A. L. Tchegotareva, M. Orrit, M. Lippitz, S. Berciaud, D. Lasne, L. Cognet, and B. Lounis, *Phys. Chem. Chem. Phys.* **8**, 3486 (2006).

Erratum: “An analytic model for the optical properties of gold” [J. Chem. Phys. 125, 164705 (2006)]

P. G. Etchegoin,^{a)} E. C. Le Ru,^{b)} and M. Meyer

The MacDiarmid Institute for Advanced Materials and Nanotechnology, School of Chemical and Physical Sciences, Victoria University of Wellington, P.O. Box 600, Wellington, New Zealand

(Received 27 September 2007; accepted 3 October 2007; published online 9 November 2007)

[DOI: 10.1063/1.2802403]

The parameters given in Table I of Ref. 1 were inadvertently obtained from a slightly different equation to Eq. 3 of Ref. 1 (and this was also used to make Fig. 1 of Ref. 1). The use of these incorrect parameters in Eq. 3 of Ref. 1 result in a reasonable representation of the optical properties of gold, but not as accurate a fit as Fig. 1 of Ref. 1 would suggest.

Table I is therefore, reproduced here for completeness with the correct parameters (to be used with Eq. 3 of Ref. 1). The corresponding fits to the optical properties of gold are shown in Fig. 1. It is clear that the fits are of the same quality as in Ref. 1, and the physical parameters of Table I do not vary significantly from those in given in Ref. 1. All the conclusions and comments of Ref. 1 are therefore completely unaffected by this change.

TABLE I. Parameters in Eq. 3 of Ref. 1 to reproduce the Johnson and Christy data (Ref. 2) shown in Fig. 1.

Parameter [units]	Johnson and Christy data (Ref. 2)
ϵ_∞	1.54
λ_p [nm]	143
γ_p [nm]	14500
A_1	1.27
ϕ_1 [rad]	$-\pi/4$
λ_1 [nm]	470
γ_1 [nm]	1900
A_2	1.1
ϕ_2 [rad]	$-\pi/4$
λ_2 [nm]	325
γ_2 [nm]	1060

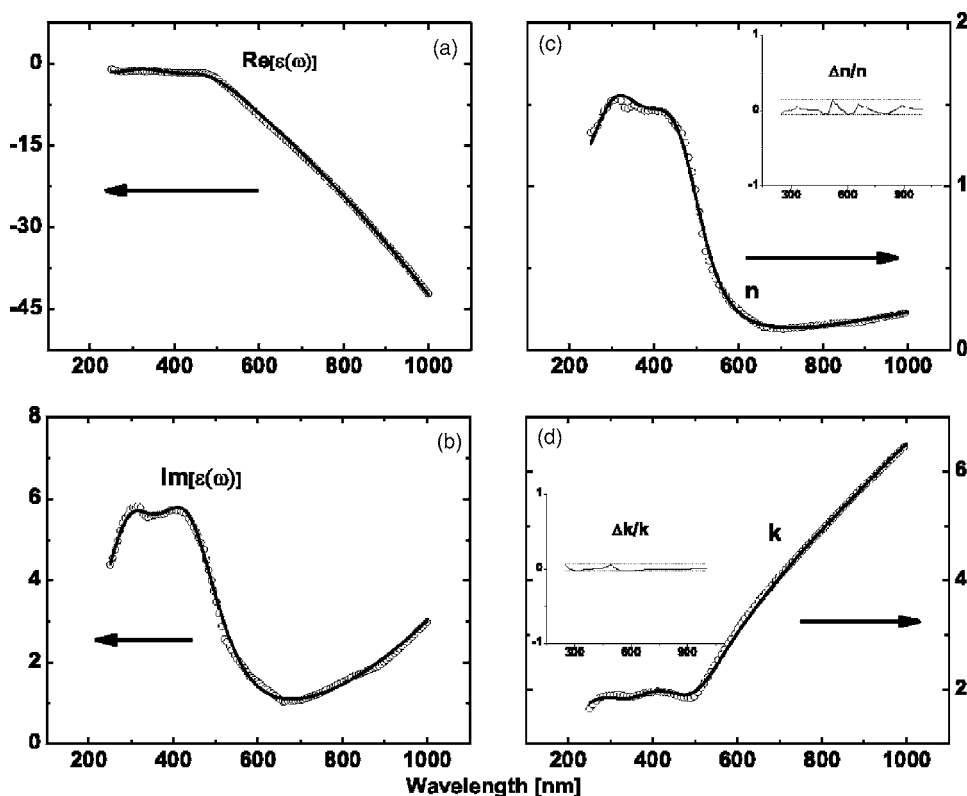


FIG. 1. (a) and (b) show the real and imaginary parts of the dielectric function of Au while (c) and (d) show the corresponding real (n) and imaginary (k) parts of the complex index of refraction. The data points are the experimental values from Johnson and Christy (Ref. 2) while the solid lines are the fitted results with Eq. 3 of Ref. 1 and the corrected parameters given in Table I of this erratum. For n and k we show the normalized spectral difference between the experimental values and the model ($\Delta n/n$ and $\Delta k/k$); the differences with the Johnson and Christy (Ref. 2) data are never higher than 14% for n and much smaller (6%) for k .

^{a)}Electronic address: Pablo.Etchegoin@vuw.ac.nz

^{b)}Electronic address: Eric.LeRu@vuw.ac.nz

¹P. G. Etchegoin, E. C. Le Ru, and M. Meyer, J. Chem. Phys. **125**, 164705 (2006).

²P. B. Johnson and R. W. Christy, Phys. Rev. B **6**, 4370 (1972).